Site occupation in the Ni-Nb μ phase

doi: 10.1103/PhysRevB.67.174203

Site occupation in the Ni-Nb μ phase

Marcel H. F. Sluiter*
Laboratory for Advanced Materials, Institute for Materials Research, Tohoku University, Sendai, 980-8577 Japan

Alain Pasturel†
Laboratoire de Physique et Modélisation des Milieux Condensés, Maison des Magistères BP 166 CNRS, 38042 Grenoble-Cedex 09, France

Yoshiyuki Kawazoe‡
Institute for Materials Research, Tohoku University, Sendai, 980-8577 Japan

(Received 8 November 2002; revised manuscript received 6 March 2003; published 22 May 2003)

The site occupation in the Ni-Nb μ phase is computed from first principles as a function of temperature and composition. It is shown that an empirical rule of thumb based on atomic size, as well as a recently formulated rule based on the approximate point group and the degeneracy of the electronic *d*-like states, can explain the gross features of the site occupations. However, neither rule explains the distinct behavior of the 12-fold-coordinated $3a$ and $18h$ sites in the μ phase. The strong Ni preference of the $18h$ site and the mixed occupancy of the $3a$ site is explained on the basis of an analysis of ordering tendencies. Predicted site occupations qualitatively agree with recent Rietveld measurements. A comparison with the compound energy model is made and the limitations of the latter are discussed.

DOI: 10.1103/PhysRevB.67.174203 PACS number(s): 64.75.+g, 61.66.Dk, 82.60.Lf, 71.20.Lp

I. INTRODUCTION

In recent years, the first-principles theory of alloy phase stability of simple crystal structures and their superstructures[1–8] has much advanced. Recently, the study of complex phases, where several inequivalent sites exist in the unit cell, has become a focus of theoretical investigations[9–16] based on the technological importance of such phases and advances in computational methods.

Much of the field of metallurgy is directly related to complex phases. Either the formation of complex phases is artfully avoided (e.g., the σ phase[17] in high-Cr steels and the μ phase[17] in Fe, Co, and Ni based superalloys) or is carefully controlled so as to produce an optimal dispersion in age hardened alloys (e.g., Al_2Cu in Al-Cu-based alloys). Increasingly, alloy design relies on semiempirical thermodynamic modeling such as in the well-known calculation of phase diagram (CALPHAD) approach.[18] The representation of complex phases in the CALPHAD framework presents special difficulties, however, because the presence of several inequivalent sites generates a large number of unknown thermodynamic parameters[19] which cannot be determined by fitting to measured thermodynamic data without knowledge of the site occupancy.[20] The occupancy of the sites can be determined with x-ray and neutron scattering techniques but this has been done for a very small number of intermetallics only. Among the most studied complex intermetallics are the σ phases, and even for these the site occupancy has been examined for a small fraction of phases only.[21] For other complex phases much less is known. Among the more than 40 known μ phases, e.g., there is only a single instance (Co-Nb) in which site occupancies have been explicitly considered.[22]

Fortunately, advances in first-principles alloy theory have made prediction of site occupation feasible. Predicted site occupancies agree well with available experimental data[9,14–16] for the few (σ) phases where such a comparison is possible, especially when full-potential electronic structure methods are used and structures are fully optimized during the computer simulation. Here, we study the Ni-Nb μ phase (see Fig. 1) for which experimental data have recently become available through Rietveld analysis of x-ray powder diffractograms.[23]

A. μ structure

The μ structure (Pearson symbol, $HR13$; Strukturbericht notation, $D8_5$; Schönflies, $R\bar{3}m$; space group, 166; prototype, Fe_7W_6) is a tetrahedral close-packed (tcp) structure of which there are many representatives.[24] Such structures are built entirely out of tetrahedral packing units,[25] which leads to characteristic Frank-Kasper polyhedra which are labeled Z12, Z14, Z15, and Z16, where the numbers refer to the coordination number of the atom centering the polyhedron. The simplest example of a tcp structure is the A15 structure which has eight atoms per unit cell. Two of these are surrounded by Z12 polyhedra, which are icosahedra, and the remaining six by Z14 polyhedra. The μ structure is rhombohedral with 5 inequivalent sites. In an idealized description of the Fe_7W_6 prototype,[26] larger W atoms occupy the sites with the highest coordination number (CN) $6c1$ (CN = 15), $6c2$ (CN = 16), and $6c3$ (CN = 14), while smaller Fe atoms occupy sites $3a$ (CN = 12) and $18h$ (CN = 12). The degeneracies refer to the hexagonal cell in which the basis is three times represented. In the prototypical A_7B_6 μ phase the smaller *A* type atom is more abundant than the larger *B* type atom. The μ phase is particularly interesting because it features all characteristic Frank-Kasper polyhedra of the tcp class of structures while the unitcell contains just 13 atoms. Other classical Frank-Kasper phases that exhibit this large

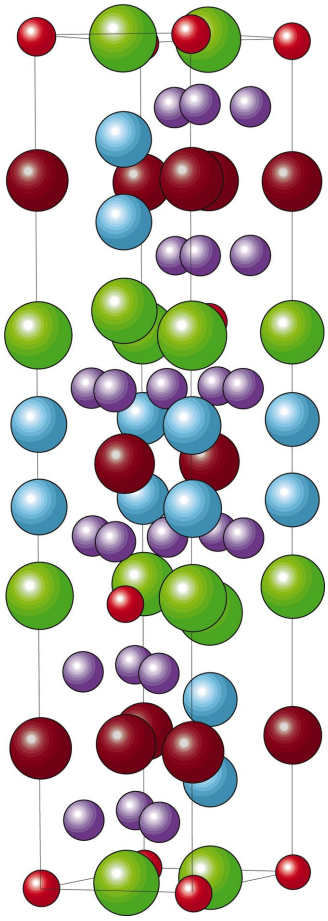

FIG. 1. (Color) Hexagonal cell of the μ phase. Top layer consists of $3a$ (small red) and $6c2$ (large green) sites; layer below, $18h$ sites (small purple); second layer below top layer, $6c3$ site (medium size light blue); third layer below, $6c1$ sites (large brown spheres).

variety have much larger unit cells, such as the δ or P phase (56 atoms per unit cell), the R phase (53 atoms per unit cell), and the exceedingly large unit cell of Cu_4Cd_3 (1124 atoms). The μ phase is of great import also because it can occur in Fe-, Co-, and Ni-based superalloys containing fourth- or fifth-row transition metals, such as the Ni-Cr-Mo alloy known as Hastelloy C-276, where μ formation substantially degrades properties.[27,28] More than 42 specific μ phases are known, many containing late third-row transition metals (Mn,Fe,Co,Ni,Cu,Zn) combined with fourth- or fifth-row transition metals, and there are a few examples involving Al or Si with transition metals.

The Ni-Nb μ phase is thus a rather representative μ structure. The Ni-Nb phase diagram[29,30] indicates the existence of the μ phase in the composition range from 49.6 to 54.5 at. % Nb. Interestingly, the larger B atomic species (Nb) is more abundant than the smaller A species (Ni) in contrast to the Fe_7W_6 prototype and this calls into question the prototypical site occupations. In other examples of the μ phase also, considerable ranges of homogeneity exist depending on the alloy system and several attempts were made to model this phase with the CALPHAD approach but the general model is still elusive.[19,31,32] The main problem in complex phases is how to model the site occupancy in the inequivalent sites as a function of composition as usually there is a lack of experimental crystallographic information as well as a lack of basic thermodynamic information. To account for the deviation from stoichiometry of the A-B μ phase in several systems, B atom occupancy on site $3a$ was considered and experimentally evidenced for example in Ni-Nb (Ref. 33) and Co-Nb (Ref. 22) systems. However, this description allows us to describe phases with compositions in the range 46.2 to 53.8 at. % B while μ phases with compositions ranging from 41 at. % (Co-Mo) to 54.5 at. % B (Ni-Ta, Ni-Nb) are known.[31] Therefore, B substitution on site $18h$ and A substitution on at least one of the sites $6c$ has been postulated in a thermodynamical treatment of this phase.[19,31,32] At present, there are no experimental data to support these assumptions.

B. Predicting site preference

Detailed theoretical predictions of site occupancy can evaluate the reasonableness of the great variety of assumed site occupancies and also allow verification of empirical models which are based on classical concepts such as atomic size and, in the case of transition metal compounds, on the concept of d-band filling. The concept of atomic size is a very tempting one because it is intuitive, and because in complex phases, unlike the previously mentioned simple crystal structures and their superstructures, there is much variation in nearest neighbor interatomic distances and coordination numbers. In the Ni-Nb μ phase, e.g., computed nearest neighbor distances range from 0.244 nm to 0.317 nm and coordination numbers range from 12 to 16.

Electronic d-like band models are semiempirical schemes[34–36] that are able to explain the basic features of transition metal alloys, such as when topologically close-packed phases are likely to occur. However, such schemes cannot generally predict which particular phase occurs[37,38] because high moments of the Hamiltonian are involved. Recently, based on a series of first-principles calculations, a rule of thumb was formulated for transition metal site occupancy based on the splitting of d-like levels depending on the coordination number.[11] The argument is that 12-fold coordinated sites often have approximately icosahedral symmetry. Such a high symmetry keeps the d-like levels close together as in the atomic case. Other coordination numbers (in topologically close-packed phases there are coordination numbers 12 or greater) invariably have lower symmetry leading to a larger splitting of d-like levels. Transition metals with approximately half-filled d bands then must shun the 12-fold-coordinated sites in favor of the other sites where the d-like bonding levels are well below the antibonding levels.

It should be emphasized that a consideration that is quite successful in ordering systems with simple crystal structures, namely optimization of the number of unlike nearest-neighbor pairs, does not work at all. For an ordering type A_7B_6 μ phase this would give rise to site occupations (probabilities of finding A atoms) of 1, 0, 0, 1, 2/3 for the sites $3a$, $6c1$, $6c2$, $6c3$, $18h$. This type of site occupancy is very

unlike the other two rules of thumb and much unlike the experimental results for the Co-Nb (Ref. 22) and Ni-Nb (Ref. 23) μ phases.

II. METHODOLOGY

The five inequivalent sites make for $2^5=32$ possible configurations of Ni and Nb atoms distributed on these sites without breaking any symmetry elements . It should be noted that these configurations are not superstructures of the μ phase because they all have the same space group. Additionally, six other configurations were considered, motivated by the fact that some sites have nearest neighbors of the same type. Pair interactions between sites of the same type can be determined only when enthalpies are available when such pairs have mixed occupancy. This required five extra configurations because there were $6c1$-$6c1$, $6c2$-$6c2$, $6c3$-$6c3$, and two distinct $18h$-$18h$ nearest-neighbor pairs. In addition there is a nearest-neighbor triangle that consists of $18h$ sites only, requiring still one more configuration.

Enthalpies of the 38 configurations have been computed within the local density approximation using the Vienna *ab initio* simulation program[39,40] (VASP) at a pressure of 0 GPa. The Kohn-Sham equations were solved with an efficient iterative matrix diagonalization scheme based on residual minimization in the direct iterative subspace[41] and optimized density mixing routines. Within this framework, the free energy is the variational functional and a fractional occupancy of the eigenstates is allowed which eliminates instabilities resulting from level crossing and quasidegeneracies in the vicinity of the Fermi level in metallic systems. The exchange-correlation functional with generalized-gradient corrections[42] is used. The calculations were performed using fully nonlocal optimized ultrasoft pseudopotentials[43] with energy cutoffs of 242 (175) eV and augmentation charge cutoff energies of 406 (340) eV for Ni (Nb). The cutoff energy for the wave functions has been set at 302 eV. The Ni (Nb) pseudopotential treats the $4s$ and $3d$ ($5s$, $4d$) like states as valence states. Integrations in reciprocal space use a $5\times5\times1$ Monkhorst-Pack[44] grid in the first Brillouin zone pertaining to the hexagonal cell, giving rise to 13 k points in the irreducible section. The Hermite-Gauss smearing method of Methfessel and Paxton[45] of order 1 has been used to accelerate k point convergence. k-point convergence was examined using $5\times5\times2$ and $6\times6\times1$ grids. After structural optimization of the pure Ni μ phase this gave rise to changes in the enthalpy of 10 meV/cell, or about 0.26 meV/atom. While much finer k-point grids might produce larger changes, these changes should be negligible for the current purpose of determining site preferences. The a and c lattice parameters of the hexagonal cell and the internal coordinates of the five inequivalent sites were optimized for all configurations using a conjugate gradient method.[39,40] Structural optimizations were considered converged when the greatest magnitude of the force on any atom was less than 1 meV/Å.

The cluster variation method[46,47] (CVM) has been used to calculate configurational thermodynamic properties. The Gibbs free energy G, expressed in term of enthalpy H, temperature T, and entropy S,

$$G=H-TS, \tag{1}$$

is minimized with respect to the configurational degrees of freedom, such as site occupancies and correlation functions. In the CVM the enthalpy and the entropy are given by a cluster expansion,

$$H^{\mathrm{CVM}}=\sum_{\alpha}^{\alpha_{\max}} J_\alpha \xi_\alpha , \tag{2}$$

$$S^{\mathrm{CVM}}=\sum_{\alpha}^{\alpha_{\max}} \gamma_\alpha S_\alpha , \tag{3}$$

where α represents a cluster, J an effective cluster interaction (ECI), ξ a correlation function, γ a Kikuchi-Barker coefficient,[47] and S_α the entropy contribution from the cluster α. $\alpha_{\max}$ represents the maximal cluster that is considered in the expansion. For a tcp phase selecting tetrahedra as maximal clusters is the most apparent choice. The maximal clusters were generated using an algorithm that searches for the most compact clusters[48] and the superiority of this maximal cluster generation method was elucidated by Vul and de Fontaine.[49] For the μ phase this algorithm gives 13 distinct tetrahedral maximal clusters and 53 clusters in total (5 points, 15 pairs, 20 triangles, and 13 tetrahedra). The entropy contributions S_α are computed from a sum over all decorations σ of cluster α,

$$S_\alpha=-\sum_{\sigma_\alpha} p_{\sigma_\alpha}\ln(p_{\sigma_\alpha}), \tag{4}$$

where p_σ is the probability for the occurrence of decoration σ. The probabilities take values between 0 and 1 and satisfy a normalization condition: $\Sigma_{\sigma_\alpha} p_{\sigma_\alpha}=1$. The probabilities are computed from the correlations functions,[47]

$$p=C\xi, \tag{5}$$

using the configuration matrix C. As the correlation functions form a complete orthonormal basis, the free energy can be conveniently minimized with respect to ξ.

For perfectly ordered configurations the correlation functions can be determined by inspection. Therefore, when the enthalpies H^s of a set of structures (s) are known, Eq. (2) can be inverted to obtain the ECI. This is the essence of the so-called Connolly-Williams method (CWM).[50,51] Here, a modified version of the CWM is used,[48] in which J_α is calculated with

$$\sum_s w^s\left[H^s-\sum_{\alpha=1}^{\alpha_{max}} J_\alpha \xi_\alpha^s\right]^2=\text{minimal}, \tag{6}$$

where w^s is the weight for each structure. The weights are determined according to

$$w^s=\left[1+w\left(\frac{d^s}{\langle d\rangle}\right)^2\right]^{-1}, \tag{7}$$

where d^s represents the enthalpy difference of a structure s to the convex hull formed by the ground state ordered struc-

TABLE I. Computed lattice parameters a and c, formation enthalpy ΔH_{form}, and internal coordinates as a function of site occupation.

Occupancy	c_{Nb}	ΔH_{form}	a	c	Internal coordinates				
a $c1$ $c2$ $c3$ h	a/o	(eV/atom)	(Å)	(Å)	z_{c1}	z_{c2}	z_{c3}	x_h	x_h
NbNbNbNbNb	1	0	5.477	28.691	0.1667	0.3333	0.4563	0.8317	0.2562
NbNbNbNbNi	0.5385	−0.3986	4.957	27.094	0.1667	0.3333	0.4516	0.8307	0.2549
NbNbNbNiNb	0.8462	0.0894	5.404	27.997	0.1667	0.3333	0.4534	0.8317	0.2528
NbNbNbNiNi	0.3846	−0.3104	4.854	26.484	0.1667	0.3334	0.4540	0.8302	0.2538
NbNbNiNbNb	0.8462	0.1696	5.368	28.452	0.1667	0.3333	0.4557	0.8300	0.2594
NbNbNiNbNi	0.3846	−0.3688	4.847	26.693	0.1666	0.3335	0.4456	0.8296	0.2576
NbNbNiNiNb	0.6923	0.2062	5.289	27.686	0.1667	0.3333	0.4544	0.8320	0.2559
NbNbNiNiNi	0.2308	−0.1958	4.730	25.965	0.1666	0.3334	0.4522	0.8288	0.2560
NbNiNbNbNb	0.8462	0.1416	5.544	27.489	0.1650	0.3333	0.4509	0.8317	0.2505
NbNiNbNbNi	0.3846	−0.2943	4.867	26.432	0.1667	0.3333	0.4519	0.8318	0.2519
NbNiNbNiNb	0.6923	−0.0100	5.373	26.660	0.1667	0.3333	0.4572	0.8317	0.2478
NbNiNbNiNi	0.2308	−0.1600	4.775	25.690	0.1666	0.3334	0.4554	0.8315	0.2496
NbNiNiNbNb	0.6923	0.3414	5.459	26.718	0.1656	0.3333	0.4534	0.8322	0.2536
NbNiNiNbNi	0.2308	−0.2865	4.741	25.886	0.1666	0.3334	0.4496	0.8301	0.2549
NbNiNiNiNb	0.5385	0.1674	5.298	25.907	0.1667	0.3333	0.4565	0.8316	0.2507
NbNiNiNiNi	0.0769	−0.0958	4.649	24.926	0.1666	0.3334	0.4536	0.8309	0.2516
NiNbNbNbNb	0.9231	−0.0254	5.532	27.366	0.1660	0.3333	0.4538	0.8327	0.2586
NiNbNbNbNi	0.4615	−0.4007	4.895	26.508	0.1646	0.3333	0.4508	0.8312	0.2575
NiNbNbNiNb	0.7692	0.0496	5.299	28.212	0.1661	0.3333	0.4545	0.8328	0.2562
NiNbNbNiNi	0.3077	−0.3791	4.789	25.829	0.1652	0.3333	0.4541	0.8319	0.2562
NiNbNiNbNb	0.7692	0.0382	5.440	27.183	0.1663	0.3333	0.4541	0.8330	0.2631
NiNbNiNbNi	0.3077	−0.2966	4.859	25.667	0.1652	0.3333	0.4445	0.8347	0.2592
NiNbNiNiNb	0.6154	0.1026	5.368	26.134	0.1660	0.3331	0.4522	0.8327	0.2589
NiNbNiNiNi	0.1538	−0.1457	4.726	24.979	0.1651	0.3333	0.4509	0.8318	0.2577
NiNiNbNbNb	0.7692	0.1121	5.520	26.425	0.1645	0.3332	0.4492	0.8312	0.2529
NiNiNbNbNi	0.3077	−0.3105	4.805	26.075	0.1655	0.3333	0.4523	0.8322	0.2553
NiNiNbNiNb	0.6154	−0.0209	5.297	27.133	0.1650	0.3333	0.4567	0.8317	0.2505
NiNiNbNiNi	0.1538	−0.2253	4.776	24.767	0.1668	0.3333	0.4541	0.8331	0.2535
NiNiNiNbNb	0.6154	0.2381	5.481	25.278	0.1667	0.3334	0.4435	0.8333	0.2574
NiNiNiNbNi	0.1538	−0.1994	4.707	25.166	0.1666	0.3333	0.4481	0.8333	0.2576
NiNiNiNiNb	0.4615	0.0625	5.275	25.364	0.1669	0.3333	0.4552	0.8331	0.2549
NiNiNiNiNi	0	0	4.624	24.194	0.1668	0.3333	0.4527	0.8331	0.2542

tures, and $\langle d \rangle$ is the enthalpy difference averaged over all structures. Of course, d^s takes the value zero if s is a ground state. w is a factor which is assigned the smallest positive value that ensures that the enthalpies of all structures are in the correct order, as in the spirit of Ref. 52. In the actual calculations w was given the value 100. Equation (6) is simultaneously under- and overdetermined. Therefore, a singular value decomposition (SVD) algorithm was used to extract values for 20 ECI out of a set of 54 using 38 enthalpies of formation, where the formation enthalpy of a structure is defined as its enthalpy minus the concentration weighted enthalpies of pure Ni and Nb with the μ structure,

$$\Delta H^{\alpha}_{\text{form}} = H^{\alpha} - c^{\alpha}_{\text{Ni}} H^{\text{Ni}-\mu} - c^{\alpha}_{\text{Nb}} H^{Nb-\mu}. \tag{8}$$

The ECI can be used to determine the enthalpy of formation of the configurationally random alloy, also known as the mixing enthalpy, because the correlation functions of the random state are given simply by products of point correlation functions. In the completely random state all sites have a probability of Nb occupancy that corresponds to the Nb concentration so that the mixing enthalpy is given by

$$H_{\text{mix}} = \sum_{\alpha}^{\alpha_{\max}} J_{\alpha} c_{\text{Nb}}^{n_{\alpha}}, \tag{9}$$

where n_{α} is the number of sites in cluster α.

III. RESULTS AND DISCUSSION

The computed crystallographic parameters and the formation enthalpies for 32 possible site occupations are listed in Table I. It is evident that site occupation has a strong effect of the lattice parameters and formation enthalpies, but has very little effect on some of the internal coordinates. In particular the z_{c1} and z_{c2} coordinates are essentially independent of site occupation and therefore also independent of composition. The remaining three internal coordinates show a little larger variation but as Fig. 2 illustrates they too vary only over a narrow range. A comparison with Rietveld re-

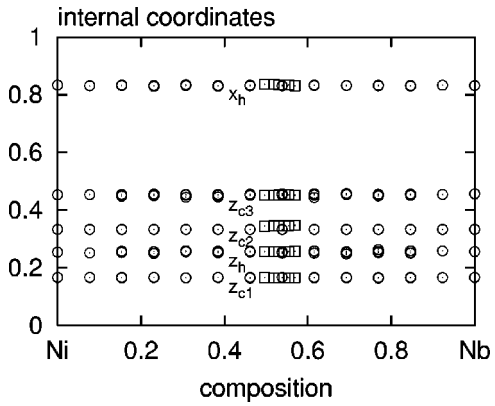

FIG. 2. Internal coordinates as a function of composition as computed (circles) and as determined by Rietveld structure refinement of x-ray data (squares) (Ref. 23).

fined x-ray measurements of Joubert and Feutelais[23] is possible over a narrow range of composition and agreement is seen to be fair. The lack of variability of the internal coordinates with respect to site occupation is very surprising when one considers the large atomic size differences and the large relaxation effects that have been measured and computed in solid solutions based on simple crystal structures, such as fcc[53,54] and diamond cubic.[8,55] However, it is completely in line with other recent calculations on the σ phase in the Re-W and Re-Ta alloy systems.[14–16] The volume of the hexagonal cell, given as $V=\frac{1}{2}a^2c\sqrt{3}$, is easily obtained from the entries in Table I and it can be compared with experimental data (see Fig. 3). While illustrating that there is good agreement between computed and measured cell volumes, more important is the compositional trend that the computed data reveal. When alloy formation is favored it is usually accompanied by a volume contraction because favorable bonds tend to be shorter. Figure 3 shows that volumes tend to be below the average for $c_{\mathrm{Nb}}<0.6$ while they are above average for alloys that are more Nb-rich. This indicates that alloy formation on the μ crystal structure is favored only for $c_{\mathrm{Nb}}<0.6$.

The ECI, obtained with Eq. (6), reproduced the formation

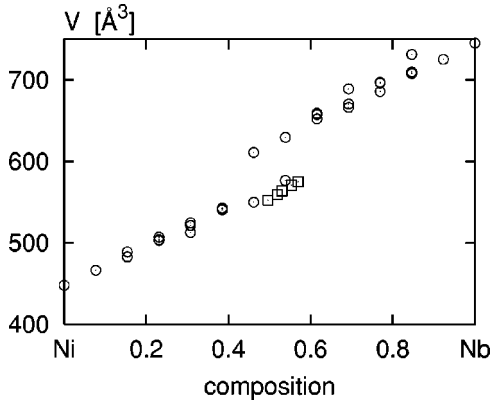

FIG. 3. Volume of hexagonal cell as a function of composition as computed (circles) and as determined by Rietveld structure refinement of x-ray data (squares) (Ref. 23).

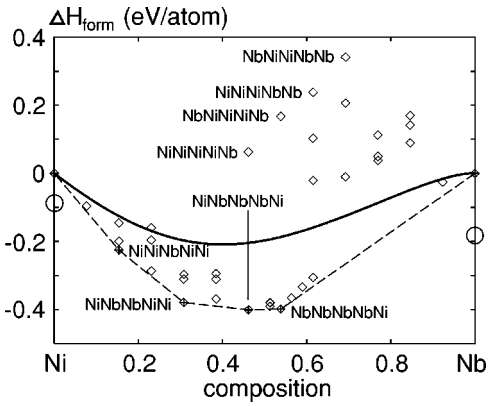

FIG. 4. Formation enthalpies as a function of the Nb concentration. The solid line indicates the enthalpy of mixing as computed with the cluster expansion [Eq. (9)]. The dashed line shows the lowest cord with the relevant ground states. Some energetically extremely unfavorable configurations are marked also. The open circle at the pure Ni (Nb) side indicates the enthalpy of the fcc (bcc) ground state.

enthalpies with a root mean square error of 22 meV/atom. This error is about the same as the smallest difference between the formation enthalpies of any of the 38 configurations used in the CWM (see Fig. 4). The predictive error[48] is a better gauge for the accuracy of a cluster expansion, and on average the enthalpy of a structure that was excluded from the cluster inversion scheme was reproduced to within 38 meV/atom, which is about 5 % of the formation enthalpy range. Experience in a variety of systems[8–10,14–16,48] has shown that such a predictive error is adequate for phase diagram calculations and site occupation determinations. Some of the higher energy structures differ less than the predictive error from each other, but near the convex hull errors due to fitting are much smaller due to the heavy weighting from Eq. (7). The results of the cluster expansion were very robust, and various changes in the way of extracting ECI's, such a changes in the assignment of weights and/or elimination of the most unstable structures, did not affect the calculated site occupation. Figure 4 shows the formation enthalpies as computed with Eq. (8) as a function of the Nb concentration. The open circles, which show the fcc Ni and bcc Nb ground state enthalpies, are at -86 and -178 meV/atom, respectively. It is evident that the μ compound near equiatomic composition is stable with respect to the pure elemental ground states. Compound formation is more favored on the Ni-rich side than on the Nb-rich side. A reason for this asymmetry is the strong Ni preference of the 18*h* site, which makes that all compounds with Nb contents greater than Ni_6Nb_7, which have Nb on the 18*h* site, are unfavorable. This is most pronounced for configurations NbNbNiNiNb (Ni_4Nb_9) and NbNiNiNiNb (Ni_6Nb_7), where the occupancy of the $3a$, $6c1$, $6c2$, $6c3$, and $18h$ sites is indicated, respectively. The large energy separation between the NbNiNiNiNb and NbNbNbNbNi configurations which have the same composition underlines the strength of the site preferences.

Another reason for the asymmetry is that ordering tendencies are intrinsically stronger at the Ni-rich side than at the Nb-rich side, as was explained by a simple rectangular

d-band model.[37] This is also evidenced by the stability of another intermetallic in the Ni-Nb system, the Ni_3Nb phase with the β Cu_3Ti-type structure. The lowest cord is shown also and going from the Nb-rich side towards the Ni-rich side the NbNbNbNbNi, NiNbNbNbNi, NiNbNbNiNi, and NiNiNbNiNi ground state configurations are encountered. Hence, the 18*h* site has the strongest preference for Ni, followed by the $3a$, $6c3$, $6c1$, and $6c2$ sites. This sequence is the same as that of the coordination numbers as one would expect on the basis of the atomic size rule of thumb which would put Ni (Nb) on the sites with the smallest (largest) coordination number.

The *d*-level splitting rule also assigns Ni, with a roughly filled *d* band, to the 12-fold-coordinated sites and Nb, with an approximately half-filled *d* band, to the 14-, 15-, and 16-fold coordinated sites. Curiously, the 12-fold-coordinated $3a$ and 18*h* sites have different attractions to the Ni species. The 18*h* site has a much stronger attraction to Ni than the $3a$ site, as is apparent from the nearly degenerate formation enthalpies of the NbNbNbNbNi and NiNbNbNbNi configurations. The atomic size rule cannot explain the difference between $3a$ and 18*h* sites because the volume around the two types of sites is the same. The *d*-level degeneracy rule also fails to explain it because the $3a$ site does not have a lower (approximate) point symmetry than the 18*h* site. In fact, the distinct behavior of $3a$ and 18*h* sites cannot be readily explained looking at single site properties such as the single site ECI. However, the $3a$ and 18*h* sites are quite distinct in terms of the number of Ni-Nb pairs that can be created.

Assuming that the $3a$ and 18*h* sites are all occupied with Ni while the remaining sites contain Nb, one could revert a single $3a$ or a single 18*h* site to Nb occupancy. In the case of the $3a$ site 0 Ni-Nb pairs would be created, while for the 18*h* site 2 Ni-Nb pairs would be lost. Ni-Nb alloys are of ordering type, as can be seen also from the negative mixing enthalpy, so that Ni-Nb pairs should be energetically favorable. It is therefore less disadvantageous to put Nb atoms on the $3a$ sites. Figure 4 reveals also that the NbNbNbNbNi and the NiNbNbNiNi configurations lower the lowest cord much more than the NiNbNbNbNi configuration because the latter is just 8.6 meV/atom below the line connecting the former two configurations. Therefore, at finite temperatures the NiNbNbNbNi configuration must be expected to disorder more rapidly than the NbNbNbNbNi and the NiNbNbNiNi configurations. This is born out by actual CVM calculations discussed below. That the mixing enthalpy should be clearly negative for a complex phase is not readily apparent, after randomly distributing large and small atoms over a set of sites with large differences in coordination number would cause large positive strain contributions.

However, the hypothetical pure Ni and pure Nb μ phases also have already large strain enthalpies built in. When the concentration-weighted strain enthalpy of the pure μ phases is subtracted from the strain enthalpy of some configurationally random μ phase, relatively little remains. This has been computed directly when it was found that enthalpies associated with structural optimization of various σ phase configurations are small and that atomic positions relax little when site occupancies are changed.[16] Hence in other ordering systems, too, negative mixing enthalpies are found on complex lattices such as that of the σ phase.[14–16]

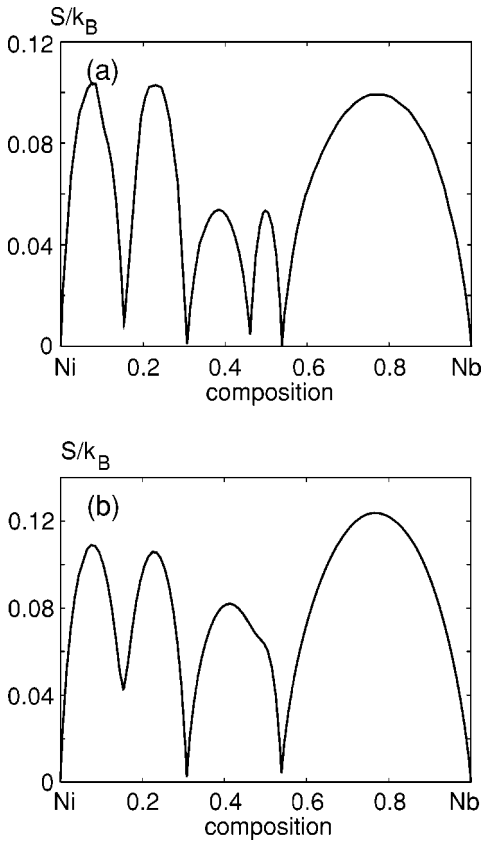

FIG. 5. Configurational entropy in the μ phase as a function of the Nb concentration at a temperature of (a) 100 K, (b) 1000 K. As Fig. 4 illustrates also, the Ni-Nb alloy on the μ lattice is of solid solution type and there are no two phase regions at temperatures of 100 K or above.

At nonzero temperature entropic effects become important, most significantly those associated with configurational disorder and vibrational excitations.[56] The configurational entropy is treated through the CVM, as expressed in Eq. (3), while the vibrational entropy has been ignored. The neglect of the vibrational entropy might cause an overestimation of the degree of order as is discussed below. In Fig. 5 the configurational entropy is shown as a function of composition at 100 K and 1000 K. At 100 K the ground state configurations can be easily recognized by the deep minima. For compositions away from the ground state configurations the occupancy on some sites is by necessity mixed, which increases the configurational entropy. As the temperature increases, ground state configurations that are only marginally more stable than their neighbors rapidly disorder. This is particularly the case for the NiNbNbNbNi configuration whose entropy minimum has faded to a mere dip. This means that in actual $Ni_{6+x}Nb_{7-x}$ μ phases, which require equilibration at high temperatures for sufficient diffusion to occur, there is significant disorder on the $3a$ sites and for very Nb-poor alloys disorder occurs even on the $6c3$ sites.

This is also evident in Fig. 6 where the probability of

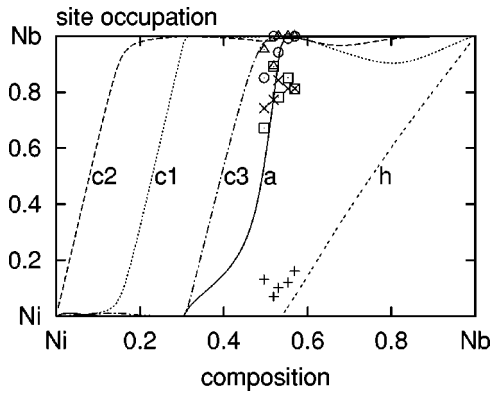

FIG. 6. Site occupancy in the μ phase at 1273 K as a function of composition; lines indicate computed results, symbols indicate Rietveld refined x-ray measurements from Ref. 23; 3*a* site (solid, $\times$), 6*c*1 site (dotted, circle), 6*c*2 site (dash, triangle), 6*c*3 site (chain-dashed, square), and 18*h* site (double dashed, $+$).

finding a Nb atom on any of the 5 sites is indicated as a function of the average composition at a temperature of 1273 K. In the range of compositions where the μ phase is observed (symbols) the 3*a* sites are clearly disordered when the Nb concentration is below 0.54. In actual $Ni_{6-x}Nb_{7+x}$ alloys on the other hand, where $c_{Nb}>0.54$, the excess Nb can be accommodated on the 18*h* sites only because all other sites are fully occupied with Nb. As was clear already from the formation enthalpies, Ni has the strongest preference for the 18*h* sites, while Nb has the strongest preference for the 6*c*2, 6*c*1, and 6*c*3 sites. The 6*c*1 site exhibits site preference reversal[9] at Nb concentrations of about 0.8, but this is far from the composition where actual μ phase occurs.

When the site preference is examined as a function of temperature a more complicated situation emerges. At composition Ni_6Nb_7 [see Fig. 7(a)] the preference seems to change with temperature. While at low temperature the Nb site preference strictly follows the coordination number of the site, at very high temperatures the 14-fold-coordinated 6*c*3 site is favored over the 16- and 15-fold-coordinated 6*c*2 and 6*c*1 sites. The reason for this can again be found in the number of Ni-Nb pairs. When the 18*h* site accepts more Nb atoms at high temperature, the 6*c*2 site, with many 18*h* nearest neighbors, loses favorable Ni-Nb pairs so it becomes energetically disadvantaged in comparison to the 6*c*3 site. It should be noted, however, that in contrast to what Fig. 6 suggests, the 6*c*1, 6*c*2, and 6*c*3 sites are seen (Fig. 7) to have similar occupancies at compositions where the μ phase has been observed. At composition $Ni_{6.5}Nb_{6.5}$ [see Fig. 7(b)] the same change in preference appears. This particular composition forces the 3*a* site to be of mixed occupancy, when the temperature is raised the Nb occupancy of the 3*a* site first increases and then very slowly decreases.

This is another instance of the site preference reversal phenomenon that was predicted for various σ phases as well.[9,14–16] It is caused by the competition of single site and multisite ECI's.[9,14–16] A comparison with experimental site occupations has become possible through the recent Rietveld studies of Joubert and Feutelais[23] The measured site occupations match well with the theoretical results in that the *c* sites

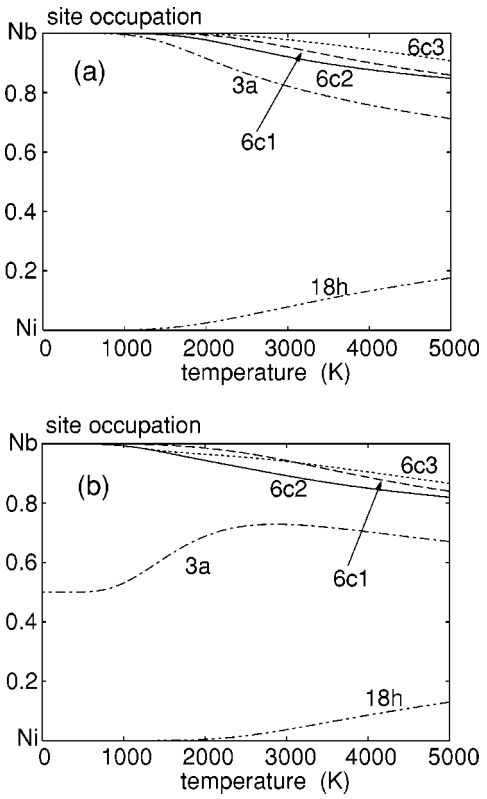

FIG. 7. Computed occupancy (Ref. 57) of the inequivalent sites in the μ phase as a function of temperature (K): (a) composition Ni_6Nb_7, (b) composition $Ni_{6.5}Nb_{6.5}$; line types as in the previous figure.

all behave rather similar with high Nb occupancy, the 3*a* site is of mixed type and the 18*h* site has a strong preference for Ni. However, to get quantitative agreement, it appears that theoretical temperatures of 2000–3000 K are required while the experimental samples were equilibrated at 1273 K. Hence, either the experimental samples have not reached equilibrium after the 10 to 30 days anneal, or the theoretical calculation underestimates entropic effects. We suspect the latter because vibrational effects have been ignored. Vibrational effects play a significant role even in alloys based on simple crystal structures,[56] and in complex crystal structures we expect an even stronger role of vibrational excitations. While locating small (large) atoms in sites with low (high) coordination numbers minimizes the enthalpy at low temperatures, at high temperatures ''wrong'' configurations with small (large) atoms in sites with high (low) coordination numbers gives rise to very negative vibrational free energies due to the easy motion of the smaller atoms in the large cages. Hence, vibrational excitations must generally be expected to promote disordering in complex phases. Currently, work is in progress to verify this hypothesis.[58]

Recently, it has been claimed[20] that the widely used compound energy model[59] (CEM) can reproduce the results of the cluster expansion—CVM approach used here. While this appears correct for the gross features it is of interest to examine the differences in these two methods a little more closely to better appreciate the power of the CEM and its limitations. In the CEM a number of simplifications are

made in the description of the configurational thermodynamics as compared to the cluster expansion—CVM approach taken here. First, the only optimization variables for the free energy are the site occupations c_i; correlations of pair, triangle, and four-body type are discarded. Second, it is usually assumed that mixing occurs on a few sublattices only and that on the remaining sublattices the occupancy is pure *A* or *B*. This assumption reduces the number of degrees of freedom and might be justified because in actual alloys the composition of complex phases is confined to some limited range. Third, the configurational entropy is assumed to be the ideal entropy of mixing, constrained by the site occupations on each sublattice *i* [e.g., see Eq. (3) in Ref. 20]. The configurational enthalpy is approximated as a polynomial in the site occupation variables,

$$\Delta H_{\text{form}} = h_0 + \sum_i h_i c_i + \sum_{i,i'}{}' h_{i,i'} c_i c_{i'} + \cdots, \qquad (10)$$

where the prime in the summations indicates that the sum is restricted to distinct indices, $i \neq i'$. The prime in the sums indicates that the highest power of the site occupations in Eq. (10) is equal to the number of inequivalent sites n_i. In the case of the μ phase $n_i = 5$. h represents coefficients that are obtained from the enthalpies of formation of all the 2^{n_i} possible ordered configurations. They are obtained conveniently from

$$h_0 = \Delta H(\sigma_j = -1),$$

$$h_i = \sum_{\sigma_i} \sigma_i \Delta H(\sigma_j = -1, \sigma_i), \quad j \neq i,$$

$$h_{i,i'} = \sum_{\sigma_i, \sigma_{i'}} \sigma_i \sigma_{i'} \Delta H(\sigma_j = -1, \sigma_i, \sigma_{i'}),$$

$$j \neq i, \quad j \neq i', \quad i \neq i' \qquad (11)$$

where σ_i indicates the occupancy of site *i*, it takes the value 1 (-1) when the site is occupied by an *A* (B) atom. It is clear that when *ab initio* values for $\Delta H(\sigma_i)$ are used the enthalpy of formation as computed with the CEM is similar to that from the cluster expansion method because the enthalpy of formation follows the same convex hull.

Of course, the cluster expansion–CVM approach can include additional structures and thereby incorporate effects that are associated with interactions between sites of the same type. In the μ phase there are nearest neighbor pairs between $6c1$-$6c1$, $6c2$-$6c2$, $6c3$-$6c3$ and two distinct $18h$-$18h$. The energetics of such pairs cannot be accounted for in the CEM while it presents no difficulties for the cluster expansion method. As the cluster expansion method incorporates arbitrary numbers and types of effective interactions and can be made arbitrarily accurate it should be considered as a generalization of the simpler compound energy model. Fortunately, it appears that for complex structures such as the σ and μ phases the 2^{n_i} values of $\Delta H(\sigma_i)$ can give a reasonable representation of the configurational formation enthalpy[9,14–16,20] because the pair interactions between same-type sites are rather small. This explains the similarity in the formation enthalpy as computed by both methods using the same set of ab initio data. However, while *ab initio* methods can provide the large number of $\Delta H(\sigma_i)$ required for the determination of *h*, this is impossible when fitting to experimental data is performed. Then, the number of parameters must be reduced by making additional assumptions. A common assumption is that some sublattices are completely occupied with one species only leaving only one or more sublattices of mixed type. Based on Fig. 6 for the μ phase one might assume that the $18h$ site is fully occupied by Ni atoms, the $6c1$, $6c2$, and $6c3$ sites take exclusive Nb occupancy and the $3a$ sites is of mixed type. It is then of some interest to compare some thermodynamic variables to examine the effect of these simplifications.

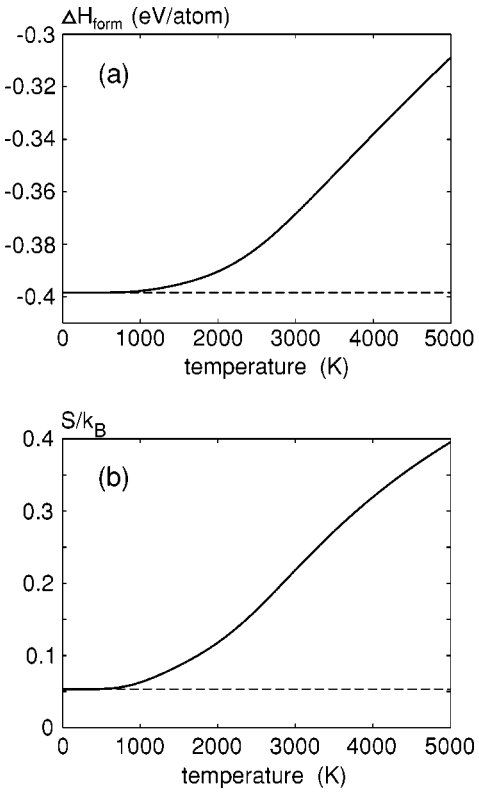

FIG. 8. Thermodynamic properties (Ref. 57) of the $Ni_{6.5}Nb_{6.5}$ μ phase as a function of temperature as computed with the cluster expansion–CVM method (thick solid lines) and as computed with the compound energy model (dashed lines) under the assumption that the $3a$ sites only are of mixed type: (a) formation enthalpy, (b) configurational entropy.

In Fig. 8 the enthalpy of formation and the configurational entropy are shown as computed by the cluster expansion–CVM approach and as computed by the CEM with the simplifications mentioned. Clearly, the simplifications have a profound effect on the temperature-dependent part of the enthalpy and entropy. Making fewer simplifications, such as allowing several mixed sublattices instead of just one, improves the agreement, but even when all sublattices are allowed to be mixed certain features that rely on pair or higher-order interactions, such as subtle composition dependent effects, are not described, e.g., see Fig. 1(b) in Ref. 20

and compare with Fig. 3 in Ref. 14. It should be remarked, however, that subtle composition-dependent occupation effects may occur beyond the narrow existence ranges or at temperatures where diffusion is so limited as to make these effects unobservable. The use of the ideal entropy of mixing in the CEM is another approximation, as Fig. 5 illustrates for the case where mixing is limited to just one sublattice in the CEM. When mixing on all sublattices is allowed, the ideal entropy is always an overestimation of the true entropy and, assuming that the enthalpy is accurately represented, it thereby leads to underestimation of the degree of site preference. This may actually appear to give better agreement with experiment because the vibrational entropy, which is neglected in the current treatments, is expected to lower the site preference at elevated temperature. Although the CEM may generally fail to describe subtle effects caused by competition between on-site and pair interactions, it generally should reproduce the enthalpy of formation well provided that the pair and higher-order interactions between sites of the same type are negligible. This can be expected for complex phases where there are relatively few such interactions, or where same-type sites are rather far apart, but it may fail for structures such as $A15$ where interactions between same-type sites can give rise to completely new ground states.[60]

IV. SUMMARY

It has been shown that the site preference of transition metals in a typical Frank-Kasper phase can be modeled using standard electronic density functional methods combined with the cluster expansion–cluster variation method. The site preference of Ni and Nb for the Z12, Z14, Z15, and Z16 coordinated sites in the Ni-Nb μ phase was found to be well described both by the empirical atomic size argument and the rule of thumb based on *d*-band filling. The small Ni atom with a filled *d* band preferred the site with the lowest coordination number and the highest approximate point symmetry, while the large Nb atom with a roughly half filled *d* band preferred the site with the highest coordination number and the lowest approximate point symmetry. The computed site preferences also agree qualitatively with those determined in actual alloys with the Rietveld method.[23]

None of the three rules of thumb can explain the strong preference of Ni for the 18*h* over the equally coordinated 3*a* site. However, it was shown that the preference for the 18*h* site could be well understood when the nearest-neighbor pairs were counted and the ordering nature of the alloy was considered. This means that the ''single-site'' type rules of thumb need to be augmented by considerations of the nearest-neighbor environment.

Contrary to solid solutions based on simple crystal structures, relaxation plays a negligible role in site preference in the Ni-Nb μ phase, as was evidenced by the site occupation independence of the internal coordinates. This surprising finding was also found for the ReW and ReTa σ phases and maybe common in tcp phases.

The widely used compound energy model was examined. It was shown to be a simplification of the cluster expansion–CVM approach used here. The compound energy model has the desirable feature of simplicity but it may become inaccurate when site occupations are idealized too much, or when there are significant interactions between sites of the same type.

ACKNOWLEDGMENTS

This work was performed under the interuniversity cooperative research program of the Laboratory for Advanced Materials, Institute for Materials Research, Tohoku University. The authors gratefully acknowledge N. Dupin and J.M. Joubert for sharing results prior to publication, and acknowledge S. Fries for suggesting this study. The authors gratefully acknowledge the Center for Computational Materials Science at the Institute for Materials Research for allocations on the Hitachi SR8000 supercomputer system (M.S.) and PHYNUM at LPMMC for computational resources on the PC cluster (A.P.).

*Electronic address: marcel@imr.edu
†Electronic address: Alain.Pasturel@grenoble.cnrs.fr
‡Electronic address: kawazoe@imr.edu

[1] G. M. Stocks, D. M. Nicholson, W. A. Shelton, B. L. Gyorffy, F. J. Pinski, D. D. Johnson, J. B. Staunton, B. Ginatempo, P. E. A. Turchi, and M. Sluiter, in *Statics and Dynamics of Alloy Phase Transformations*, edited by P. E. A. Turchi and A. Gonis, NATO ASI Series B: Physics (Plenum, New York, 1994), Vol. 319, p. 305.
[2] M. Sluiter, D. de Fontaine, X. Q. Guo, R. Podloucky, and A. J. Freeman, Phys. Rev. B **42**, 10 460 (1990).
[3] V. Ozolins, C. Wolverton, and A. Zunger, Phys. Rev. B **57**, 6427 (1998).
[4] D. Morgan, A. van de Walle, G. Ceder, J. D. Althoff, and D. de Fontaine, Modell. Simul. Mater. Sci. Eng. **8**, 295 (2000).
[5] M. Asta, V. Ozolins, and C. Woodward, JOM **53**, 16 (2001).
[6] T. Mohri and Y. Chen, Mater. Trans., JIM **43**, 2104 (2002).
[7] Y. Chen, T. Atago, and T. Mohri, J. Phys.: Condens. Matter **14**, 1903 (2002).
[8] M. Sluiter and Y. Kawazoe, Mater. Trans., JIM **42**, 2201 (2001).
[9] M. H. F. Sluiter, K. Esfarjani, and Y. Kawazoe, Phys. Rev. Lett. **75**, 3142 (1995).
[10] M. Sluiter, M. Takahashi, and Y. Kawazoe, J. Alloys Compd. **248**, 90 (1997).
[11] C. Berne, A. Pasturel, M. Sluiter, and B. Vinet, Phys. Rev. Lett. **83**, 1621 (1999).
[12] C. Berne, A. Pasturel, M. H. F. Sluiter, and B. Vinet, Modell. Simul. Mater. Sci. Eng. **8**, 233 (2000).
[13] C. Wolverton and V. Ozolins, Phys. Rev. Lett. **86**, 5518 (2001).
[14] C. Berne, M. H. F. Sluiter, Y. Kawazoe, and A. Pasturel, J. Phys.: Condens. Matter **13**, 9433 (2001).
[15] C. Berne, M. H. F. Sluiter, and A. Pasturel, J. Alloys Compd. **334**, 27 (2002).
[16] C. Berne, M. Sluiter, Y. Kawazoe, T. Hansen, and A. Pasturel, Phys. Rev. B **64**, 144103 (2001).
[17] J. L. C. Daams, P. Villars, and J. H. N. van Vucht, *Atlas of Crystal Structures for Intermetallic Phases* (ASM International, Materials Park, Ohio, 1991), p. 3804.

[18] N. Saunders and A. P. Miodownik, *Calphad*, Pergamon Materials Series Vol. 1, edited by R. W. Cahn (Pergamon, New York, 1998).
[19] I. Ansara, T. G. Chart, A. Fernandez Guillermet, F. H. Hayes, U. R. Kattner, D. G. Pettifor, N. Saunders, and K. Zeng, CALPHAD: Comput. Coupling Phase Diagrams Thermochem. **21**, 171 (1997).
[20] S. G. Fries and B. Sundman, Phys. Rev. B **66**, 012203 (2002).
[21] P. Villars and L. D. Calvert, *Pearson's Handbook of Crystallographic Data for Intermetallic Phases*, 2nd ed. (ASM International, Materials Park, Ohio, 1991).
[22] V. Wagner, M. Conrad, and B. Harbrecht, Acta Crystallogr., Sect. C: Cryst. Struct. Commun. **51**, 1241 (1995).
[23] J.-M. Joubert and Y. Feutelais, CALPHAD: Comput. Coupling Phase Diagrams Thermochem. **26**, 427 (2002).
[24] C. B. Shoemaker and D. P. Shoemaker, in *Developments in the Structural Chemistry of Alloy Phases*, edited by B. C. Giessen (Plenum, New York, 1969), p. 107.
[25] A. K. Sinha, Prog. Mater. Sci. **15**, 79 (1972).
[26] H. Arnfelt, Jernkontorets Ann. **119**, 185 (1935), as quoted in Ref. 17.
[27] Raghavan Ayer, J. C. Scanlon, M. Watkins, G. A. Vaughn, and J. W. Steeds, J. Mater. Res. **3**, 1 (1988).
[28] J. R. Crum, W. Ona, J. M. Poole, and E. L. Hibner, (To Inco Alloys International, Inc.), European Patent No. EP 0 392 484 B1, Aug. 12 (1998).
[29] H. Okamoto, J. Phase Equilib. **13**, 444 (1992).
[30] A. Bolcavage and U. Kattner, J. Phase Equilib. **17**, 92 (1996).
[31] K. C. Hari Kumar, I. Ansara, and P. Wollants, CALPHAD: Comput. Coupling Phase Diagrams Thermochem. **22**, 323 (1998).
[32] I. Ansara, B. Burton, Q. Chen, M. Hillert, A. Fernandez Guillermet, S. G. Fries, H. L. Lukas, H. J. Seifert, and W. A. Oates, CALPHAD: Comput. Coupling Phase Diagrams Thermochem. **24**, 19 (2000).
[33] P. I. Kripyakevitch, E. I. Gladyshevskii, and E. N. Pylaeva, Sov. Phys. Crystallogr. **7**, 165 (1962).
[34] R. E. Watson and L. H. Bennett, Acta Metall. **32**, 477 (1984).
[35] P. E. A. Turchi, G. Treglia, and F. Ducastelle, J. Phys. F: Met. Phys. **13**, 2543 (1983).
[36] R. Phillips and A. E. Carlsson, Phys. Rev. B **42**, 3345 (1990).
[37] M. Sluiter, P. Turchi, and D. de Fontaine, J. Phys. F: Met. Phys. **17**, 2163 (1987).
[38] P. E. A. Turchi, *Cluster and Cluster-assembled Materials*, edited by R. S. Averback, D. L. Nelson, and J. Bernholc, Mater. Res. Soc. Symp. Proc. Vol. 206 (Materials Research Society, Pittsburgh, Pennsylvania, 1991), p. 265.
[39] G. Kresse and J. Furthmüller, Comput. Mater. Sci. **6**, 15 (1996).
[40] G. Kresse and J. Furthmüller, Phys. Rev. B **54**, 11 169 (1996).
[41] P. Pulay, Chem. Phys. Lett. **73**, 393 (1980).
[42] J. P. Perdew and Y. Wang, Phys. Rev. B **45**, 13 244 (1992).
[43] G. Kresse and J. Hafner, J. Phys.: Condens. Matter **6**, 8245 (1994).
[44] H. J. Monkhorst and J. D. Pack, Phys. Rev. B **13**, 5188 (1976).
[45] M. Methfessel and A. T. Paxton, Phys. Rev. B **40**, 3616 (1989).
[46] R. Kikuchi, Phys. Rev. **81**, 988 (1951).
[47] D. de Fontaine, in *Solid State Physics*, Vol. 34, edited by H. Ehrenreich, F. Seitz, and D. Turnbull (Academic Press, New York, 1979), p. 73.
[48] M. H. F. Sluiter, Y. Watanabe, D. de Fontaine, and Y. Kawazoe, Phys. Rev. B **53**, 6137 (1996).
[49] D. A. Vul and D. de Fontaine, in *Materials Theory and Modelling*, edited by J. Broughton, P. D. Bristowe, and J. M. Newsam, MRS Symposia Proceedings No. 291 (Materials Research Society, Pittsburgh, 1994), p. 401; D. de Fontaine, in *Solid State Physics*, edited by H. Ehrenreich and D. Turnbull (Academic Press, New York, 1994), Vol. 47, p. 84.
[50] J. W. D. Connolly and A. R. Williams, Phys. Rev. B **27**, 5169 (1983).
[51] D. de Fontaine, in *Solid State Physics*, Vol. 47, edited by H. Ehrenreich and D. Turnbull (Academic Press, New York, 1994), p. 80.
[52] G. D. Garbulsky and G. Ceder, Phys. Rev. B **51**, 67 (1995).
[53] G. Renaud, N. Motta, F. Lancon, and M. Belakhovsky, Phys. Rev. B **38**, 5944 (1988).
[54] N. Mousseau and M. F. Thorpe, Phys. Rev. B **45**, 2015 (1992); L. G. Ferreira, V. Ozolins, and A. Zunger, *ibid.* **60**, 1687 (1999).
[55] I. Yonenaga and M. Sakurai, Phys. Rev. B **64**, 113206 (2001), and references therein.
[56] A. van de Walle and G. Ceder, Rev. Mod. Phys. **74**, 11 (2002).
[57] The $3a$ site occupation does not approach 0 or 1 and the entropy does not approach 0 as should occur in actual alloys on the basis of the third ''law'' of thermodynamics. This is due to the short-ranged nature of the interactions in our model. In real alloys the ECI are not strictly zero beyond the short range considered here and as a result in actuality the $3a$ sites are not energetically isolated from each other. Such interactions between $3a$ sites forbid disorder on the $3a$ sites below some nonzero temperature. A good illustration of the effect of longer-ranged interactions on the phase diagram at low temperature can be found in Ref. 60.
[58] M. H. F. Sluiter, Y. Kawazoe, and A. Pasturel (to be published).
[59] B. Sundman and J. Agren, J. Phys. Chem. Solids **42**, 297 (1981).
[60] P. E. A. Turchi and A. Finel, Phys. Rev. B **46**, 702 (1992).